HISTORIC CLIMATE VARIABILITY OF WETNESS IN EAST CHINA (960–1992): A WAVELET ANALYSIS

JIANMIN JIANG[1]*, DE'ER ZHANG[2] AND KLAUS FRAEDRICH[1]

[1]*Meteorologisches Institut, Universität Hamburg, Bundesstrasse 55, D-20146, Hamburg, Germany*
[2]*National Climate Center, Beijing, 100081, People's Republic of China*
email: fraedrich@dkrz.de

ABSTRACT

Temporal and spatial climate variability in East China is analysed for the last 1033 years (AD 960–1992) based on historic annual grades of wetness for six regions in East China. This data set is subjected to a 'Mexican hat' wavelet transform for displaying variations of different frequencies at particular time points, persistent anomalies, and abrupt changes between them. The following results are noted: the persistent dry stage 1120–1220 and wet stage 1280–1390 in the coastal regions are the outstanding features during the last 1033 years. For all regions an almost synchronous change occurs around 1890 from a weaker wet phase to a weaker dry phase; climatic variations on longer time-scales cover larger areas. On shorter time-scales, synchronous fluctuations are observed in fewer years than longer time-scale variability. © 1997 by the Royal Meteorological Society. *Int. J. Climatol.*, 17: 969–981 (1997).

(No. of Figures: 7   No. of Tables: 1   No. of Refs: 28)

KEY WORDS: East China; wavelet analysis; grades of wetness.

1. INTRODUCTION

Modern research of historic climatic fluctuation in China may be traced back to Chu (1926). Chu's (or Zhu in Chinese) last paper (Chu, 1973) on this topic summarizes the long time-scale fluctuation of temperature in China during the last 5000 years. The State Meteorological Administration of China (1981) used historic documents from provinces and counties to establish 'Yearly Charts of Drought/Floods in China for the Last 500 Years (1470–1979)', and provide a data set of annual wetness grades presented in five numbers (1 to 5) at 120 stations for the China mainland for the same period. Since then a considerable number of analyses have been performed based on these data (Sheng, 1981; Wang and Zhao, 1981; Zhang, D. 1983; Zhang, J. *et al.*, 1983). Noteworthy are also Gong and Hameed (1991) reconstructing the history of conditions of wetness in East China for the last 2000 years in terms of 5-year means; Wang *et al.* (1991) reconstructing a series of the seasonal temperature grades for the last 500 years in 10-year resolution; and Fang (1992) establishing a data bank from records of climatic disasters and anomalies in ancient Chinese documents describing the earliest record of a great flood in 2597 BC and frequent records after 659 BC.

According to International Geosphere–Biosphere Programme (IGBP) objectives, Zhang *et al.* (1995) extend the series of annual wetness grades with an annual resolution back to AD 960, distinguishing six regions in East China. This data set will be analysed with the wavelet transform technique. Section 2 provides a brief description of the data set and the methodology of the wavelet transform. Results are presented in sections 3 and 4. Section 5 gives a summary.

2. DATA AND METHOD OF ANALYSIS

2.1. A brief description of the data set

From historic chronicles and documents in which drought/flood disasters are recorded, five annual grades of wetness (abnormally wet, wet, normal, dry, abnormally dry) were deduced previously at 120 stations in China

---

*Visiting Scientist. Correspondence to: Beijing Meteorological College, 46 Baishiqiaolu, Beijing, 100081, People's Republic of China.

for 1470–1949, as mentioned above. During the 30-year period 1950–1979, these wetness grades, based on the documents recording drought/floods, are related to instrumental observations of rainfall (RR) for the following five standard deviation (σ) classes of rainfall: $RR > 1.17\sigma$, $1.17\sigma > RR > 0.33\sigma$, $0.33\sigma > RR > -0.33\sigma$, $-0.33\sigma > RR > -1.17\sigma$, $-1.17\sigma > RR$ (Table I). Note that grade 3 indicates also years in which no records were found within three consecutive years, because it was customary in the historic documents to write about abnormal climate events and calamaties rather than normal situations. When no records were found for more than 3 years, each year is denoted as missing.

Six regions (Figure 1) have been selected from the regionalization by applying cluster analysis to the annual grades of wetness during the period from 1470–1979 evaluated at the 120 stations in China. This reduction of the data set to six regional time series allows a climatologically meaningful extension of the time series back to AD 960 for another half millennium when historic records of drought/floods are becoming sparser and available in fewer counties and provinces. Region 1 mainly covers the Hebei Province, Beijing, and Tianjing cities; region 2 is the Shanxi Province; region 3 represents the low part of Yellow River (Huanghe) and the Shandong Province; region 4 is the Henan Province; region 5 indicates the downs of Yangtze River (Changjiang) and the basin of Huai River (Anhui Province and the north Jiangsu Province); region 6 denotes Zhejiang Province, the southern Jiangsu Province and Shanghai city. The regional grades of wetness for the period 1980–1992 are identified basically by using rainfall standard deviation.

The six regional time series all cover a total 1033 years for the period from AD 960 to 1992, with absences of 60 years in the series of region 1, of 140 years in region 2, of 86 years in region 3, of 37 years in region 4, of 15 years in region 6, and none missing in region 5. These absences occurred mostly in the period from AD 1040 to 1259. An example of a regional time series for region 6 is shown in Figure 2(a).

Before analysing the data in more detail, the basic statistics are described first. The probability distribution of the five grades during 1260–1992 shows an almost normal distribution for all six regions (Figure 2(b)): around 32 per cent of the probability occurs on the normal grade, 23 or 22 per cent on the wet or dry grade, 12 or 11 per cent on the abnormally wet or abnormally dry grade; the wet and abnormally wet grades hold a little more probability than the dry grades. These features differ somewhat from the common use specifying 25 per cent of the probability on the normal grade, 25 per cent on the dry or wet grade, and 12·5 per cent on the abnormally dry or abnormally wet grade. The reason may be that we paid more attention to the records of historic documents and occasionally put grade 3 in years when no records were found within three consecutive years. Figures 2(c and d) presents the distribution for the semi-arid region 2 and the wet region 6. There more droughts than floods appear in region 2, which is characterized by a semi-arid climate, whereas more floods occur in region 6, which is classified as a wet climatic zone. This is basically a qualitative reflection of the non-normal distribution of local

Table I. Classification of five annual grades of wetness in East China

Grade	Name	Classification of records in historic documents	Comparison with the present[a] in standard deviation of rainfall (σ)
1	Abnormally wet	Continuously heavy rain, severe floods in large areas	$RR > 1.17\sigma$
2	Wet	Rainy, local floods	$0.33\sigma < RR < 1.17\sigma$
3	Normal	Good climate and harvest, or no records found within 3 years	$-0.33\sigma < RR < 0.33\sigma$
4	Dry	Little rain persisted within one month or one season	$-1.17\sigma < RR < -0.33\sigma$
5	Abnormally dry	Persistent droughts over more than one season	$RR < -1.17\sigma$

[a]Based on observations during the period from 1950 to 1979.
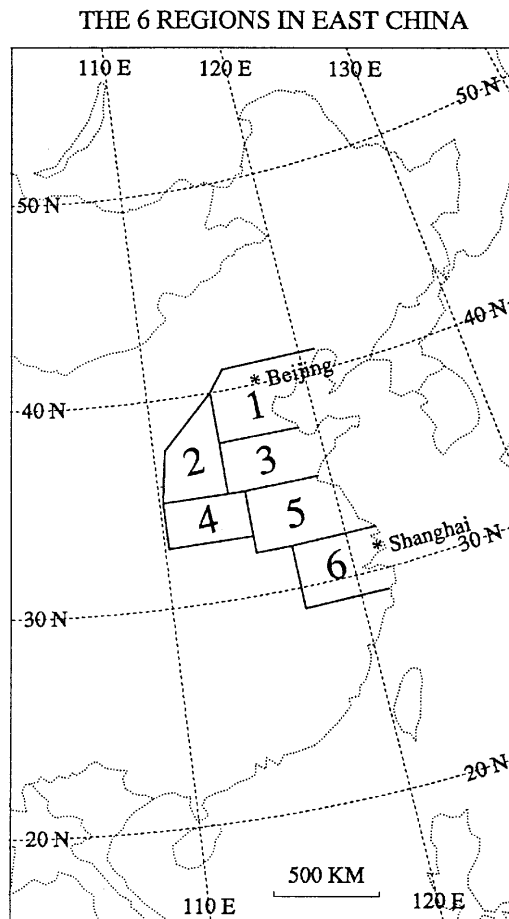
THE 6 REGIONS IN EAST CHINA

Figure 1. The six regions in East China

and regional precipitation in different climate zones. Furthermore, it appears that there is no essential difference between the former and the latter 500 years of this data series (Zhang, 1991).

2.2. Wavelet transform

The wavelet transform technique has been introduced and formulated by Morlet *et al.* (1982), and Grossmann and Morlet (1984). This analysis is applied widely in signal and image processing using various basic wavelets or 'mother wavelet' functions. In meteorology, Mahrt (1991), Kumar and Foufoula-Georgiou (1993), and Gamage and Blumen (1993) apply the orthogonal (or Haar) wavelet analysis to the research of boundary layer meteorology, rainfall processes, and cold fronts, respectively. Using the complex Morlet wavelet scheme, Spedding *et al.* (1993) and Meyers *et al.* (1993) decompose the wind-generated surface wave field at the air–sea interface, Weng and Lau (1994) analyse the organization of convection based on infrared radiance. Gao and Li (1993) apply the 'Mexican hat', now a commonly used wavelet function, to turbulence data. They have all commented on the advantages of this technique compared with the Fourier transform: the wavelet analysis shows structures on different time (or spatial) scales at different time (or spatial) locations. For more details see Foufoula-Georgiou and Kumar (1994).

The traditional Fourier transform provides information only on the frequency, without its variation in time (or position) on a single frequency in the signal series analysed. The wavelet transform provides localized time and frequency information without requiring the time series to be stationary. It transforms a one-dimensional function

a. WETNESS GRADE TIME SERIES FOR REGION 6

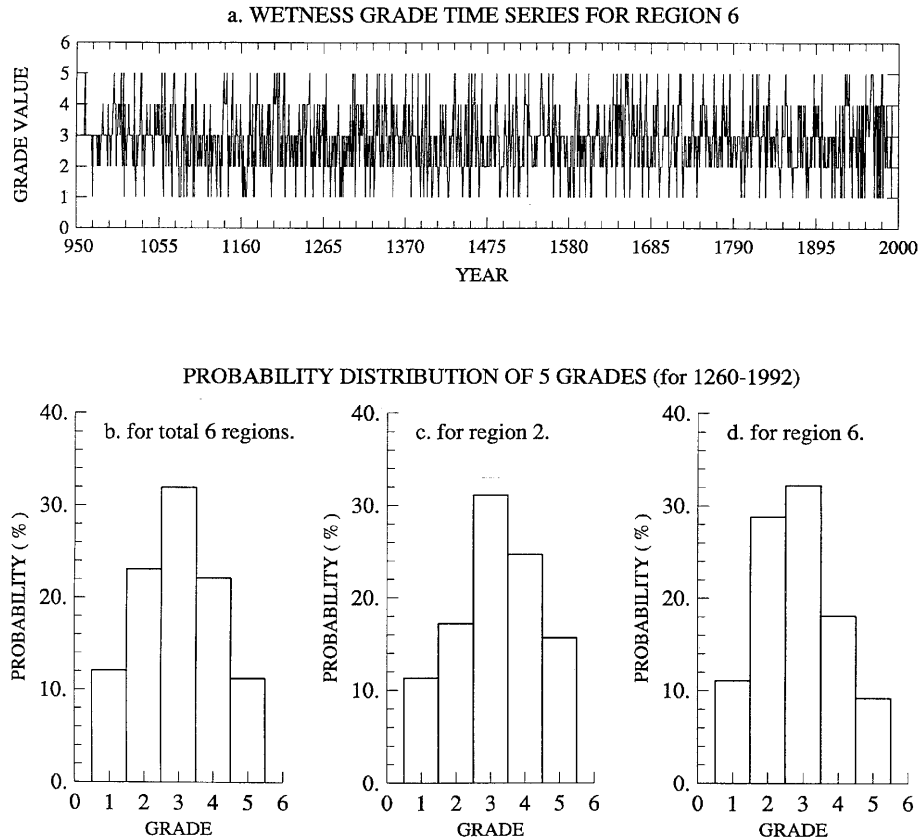## PROBABILITY DISTRIBUTION OF 5 GRADES (for 1260-1992)

Figure 2.   The regional time series for region 6 (a), and probability distribution of occurrences of the five grades during the period from 1260 to 1992: (b) for all six regions, (c) for region 2, and (d) for region 6

of time into a two-dimensional function of time and frequency or, equivalently, scale (Liu, 1994). There are two kinds of wavelet functions based on symmetric and anti-symmetric wavelets. A symmetric wavelet is the second derivative of a smoothing function and is optimal for finding maximum curvature. The 'Mexican hat' wavelet is the second derivative of the Gaussian function, and is known as being good at localization in frequency or scale (Brunet and Collinean, 1994).

In this study, we adopt the 'Mexican hat' wavelet to analyse each of the six regional time series. Details of the wavelet transform formulae and the 'Mexican hat' function are described briefly in the Appendix. According to the definition of the wavelet function, the time-scale parameter a represents the scale of the fluctuation. A smaller a value refers to a shorter scale or a higher variation frequency. In this study, a is equivalent to 1/4 cycle. The location parameter b corresponds to the time points in a year-to-year sequence. A full wavelet transform should be performed for $4a + 1 < b < N - 4a$, with $N = 1033$ for each individual region. In order to detect climatic variations on decadal and century scales, we run computations on the normalized time series of grades (by subtracting the mean and dividing by the standard deviation) with the following time-scale parameters: $a = 1, 2, 4, 8, 10, 20, 30, \ldots, 120, 130$ years, through all data points: $b = 1, 2, \ldots, N$ (i.e. AD 960–1992) because historic climatic data sets are limited. Edge effects may occur, magnifying or reducing values of the wavelet coefficients at the start and the end of the series, but the sign and other essential properties remain basically unaltered, unless an abrupt change happens. In addition, grade 3 is used for the missing data. The results presented show clear and smooth contour patterns and good localization of the time-scale (or frequency) of the variability at different time points.

The wavelet coefficients or wavelet transform function $W(a,b)$ (see equation (1) in the Appendix) in this study present wetness variations on various time-scales and at different time points (years). $W(a,b) > 0$ responds to the

dry grades and $W(a,b) < 0$ to the wet grades. The positive maximum values of $W(a,b)$ indicate severe dryness whereas the negative minima denote severe wetness. A close pair of minimum and maximum centres of $W(a,b)$ with a large gradient, may display an abrupt change from one persistent spell of anomaly to another anomaly of opposite sign, leaving the required significance threshold as an open question (Brunet and Collinean, 1994).

3. VARIABILITY OF LONG AND SHORT TIME-SCALES IN INDIVIDUAL REGIONS

From the wavelet transform of all six regions, we select regions 3 and 6 to show different variabilities on long and short time-scales, a, changing as time progresses, b. Region 3 (Figure 3(a) shows significant variations on longer time-scales, $50 < a < 100$ years, where a corresponds to 1/4 cycle. Note that the ratio of the scale parameter a and the period of cycles depends on the mother wavelet function. Furthermore, the periodicity and the intensity of the variations change with the time parameter b in wavelet transform. The following results are noted: (i) the time-scale or the period of variability becomes longer from 1020 to 1767. This feature is denoted by the extreme centres of $W(a,b)$ located on the 30-year scale around 1020, the 60-year scale in 1202, the 75-year scale in 1328, the 90-year scale in 1496, and up to longer than 130-year scale around 1767. (ii) The intensity of variations appears to be much stronger around 1328 and 1496 than that in 1095 and 1767. The intensities of $W(a,b)$ at the extreme centres are $-2 \cdot 0$ in 1328, $+1 \cdot 75$ in 1496, whereas about $-0 \cdot 25$ without a significant centre around 1095, and $-1 \cdot 25$ on the 130-year scale in 1767. Note that these time-scale (or frequency) features cannot be revealed by the Fourier transform. (iii) There are relatively *dry* periods on the 60-year scale between 1139 and 1260 and on the 90-year scale from 1410 to 1602, in which $W(a,b) > 0$ (solid lines); the *wet* periods with $W(a,b) < 0$ (dashed lines) are noted on the 75-year scale from 1260 to 1409 and on the 130-year scale from 1655 to 1895. These results are consistent with Gong and Hameed's (1991) analysis for a region corresponding to our region 3. There are, however, differences to their results in the first 100 years from 960 to 1060. (iv) Moreover, there are three abrupt changes from a persistent dry spell to a wet one around 1260 on the century fluctuation scale of a ca. 80 years, and a reverse change around 1345 on the 30-year scale, and another reverse again around 1540 on the 50-year scale. Other significant abrupt changes on shorter time-scales, such as around 1460 on the 25-year and 1775 on the 20-year scales, are marked in Figure 3(a) by pairs of dominant $W(a,b)$ centres of opposite sign, which are close to each other with a large gradient across the zero line. These abrupt climate changes were also identified by a moving Student's t test applied to detect the difference of subsample means between two adjoining subsamples in the same time series using a subsample size of 75 years and 15 years (Zhang and Jiang, 1996).

Unlike region 3 with its long time-scale variability, region 6 (Figure 3(b)) shows fluctuations on shorter time-scales, $30 < a < 40$ years. The time-scale of most pronounced variations reduces from 65 years to 25 years during the years 1020 to 1685. Note that the edge effect of the wavelet transform at both ends of the series is limited to fewer years, which is due to the short scales involved. Most of the dry spells, 1180–1245, 1328–1380, 1520–1565 and 1635–1670, and wet episodes, 1245–1300, 1570–1610 and 1875–1920, coincide roughly with Gong and Hameed's (1991) analysis of the similar region; again the first 100 years are different. An abrupt change from a dry spell to a wet episode (on the time scale $a = 20$–30 years) and a reverse change are observed around 1565 and 1635, respectively. The latter was also detected by the 't' test using a subsample size of 15 years (Zhang and Jiang, 1996).

4. REGIONAL ANALYSIS

Wavelet variance (equation (6) in the Appendix) is a measure of the wavelet spectrum and is proportional to the energy of the signal (Hagelberg and Gamage, 1994). Figure 4 shows wavelet variances for time-scales $a > 10$ years for all regions. The variations with peaks of variance on longer time-scales, $a = 70$–90 years, are prominent in regions 1, 3 and 5, whereas those with peaks on shorter time-scales, $a = 10$–40 years, are dominant in regions 2, 4 and 6, although every region shows different peak time-scales. The common ground and differences of climatic fluctuations in these regions are expanded and analysed next.

To analyse links between the climate variabilities in the six regions, we present the regional-time evolution by applying the wavelet expansion (equation (8) in the Appendix) on the two distinctly different time-scales

WAVELET TRANSFORM FOR REGION 3
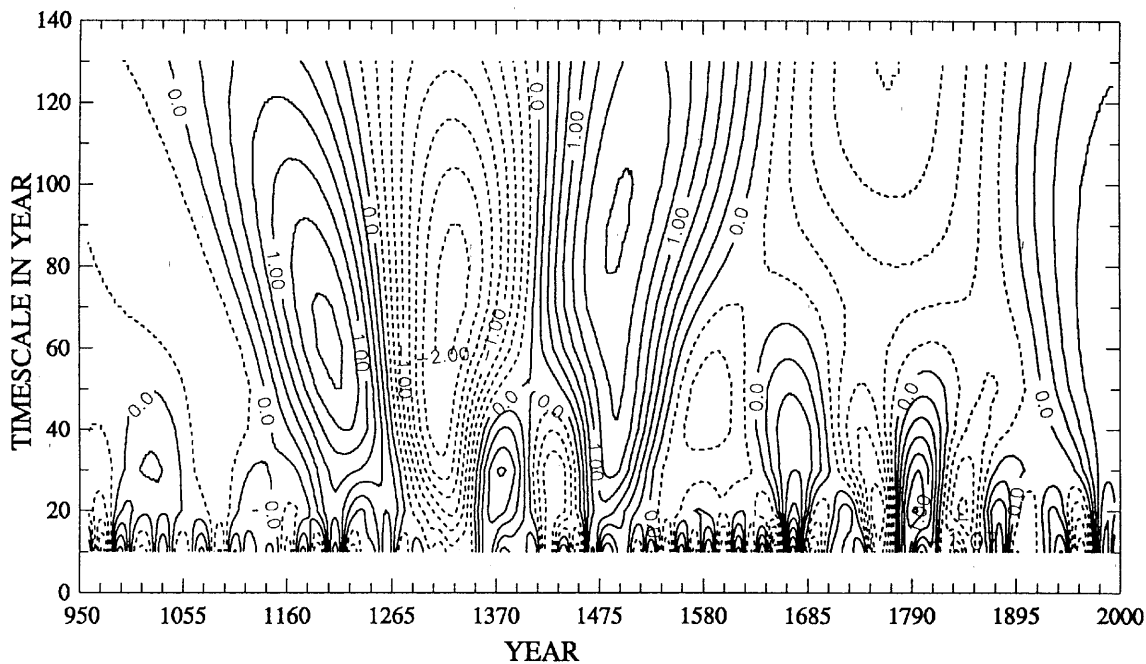
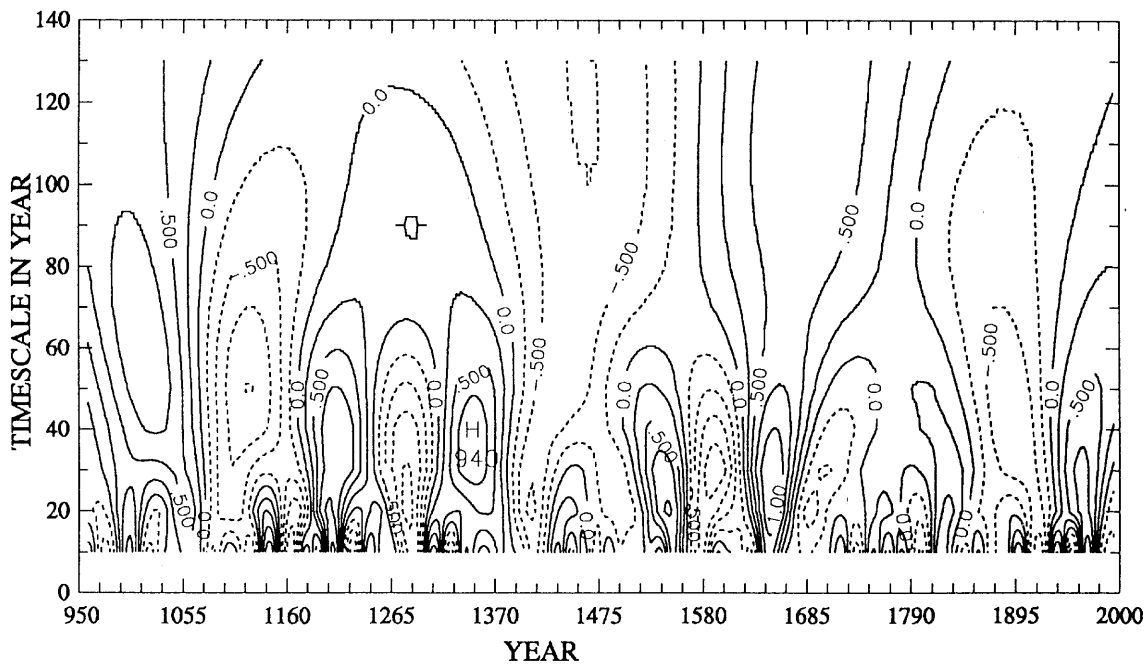## WAVELET TRANSFORM FOR REGION 6

Figure 3. The wavelet transform of wetness grade series: for region 3 (top) and region 6 (bottom)

identified above, $a = 80$ and $a = 10$ years. In addition, we 'zoom in' on a couple of segments at the $a = 2$ years time-scale.

Note that the wavelet expansion $y(a,t)$ is an output of a linear filter, using the wavelet function as a filter on a given (single) scale. Compared with the Fourier expansion, this is a decomposition of the wavelet. The values of the expansion $y(a,t)$ are measures of the wetness grades, with features similar to the wavelet transform $W(a,b)$.

The wavelet expansion on the long time-scale $a = 80$ years shows synchronism in regions 5, 3, 1, 4 and 2, with a slight shift from south to north before 1450 (Figure 5, the vertical axis is arranged to correspond to the regions 6, 5, 3, 1, 4 and 2 to make this feature more visible). The following results are summarized: (i) there are three pairs of wet and dry stages. The comparatively wet climate background is observed during 960–1100, 1265–1410, and 1650–1875, with severe wet years around 990–1010 in regions 5 and 1, and 1305–1325 in region 3. The relatively dry climates occur in 1100–1265, 1410–1650, and after 1875, with severe dry years around 1120–1140 in regions 5 and 1, and around 1495 in region 3. (ii) An outstanding change from a dry phase to a wet stage occurred around 1265 in regions 1, 3 and 5, which is marked by the large gradient of the expansion values across the zero line from high positive to minimum negative. This is also consistent with the detection by Zhang and Jiang (1996). This period corresponds to the 'little or secondary climate warm epoch' in Europe (Hassan, 1981). In addition, reverse changes around 1412 from a wet spell to a dry episode in region 3 and around 1070 in region 5 are also apparent. (iii) Region 2 follows after 40–80 years of being weaker (which includes the influence of missing data); whereas region 6 fluctuates much more weakly and with almost opposite phase. (iv) However, after the seventeenth century, around 1890, a slow synchronous change from a weaker wet stage to a weaker dry phase is obvious in East China, but it is somewhat delayed in region 6.
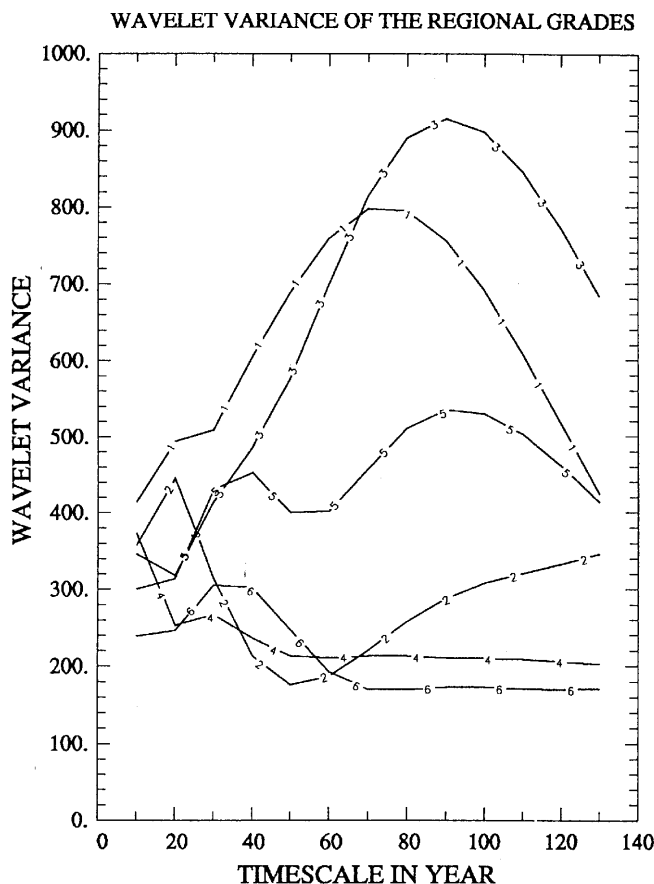

Figure 4.   The wavelet variances for the six regions. The curves 1 to 6 indicate regions
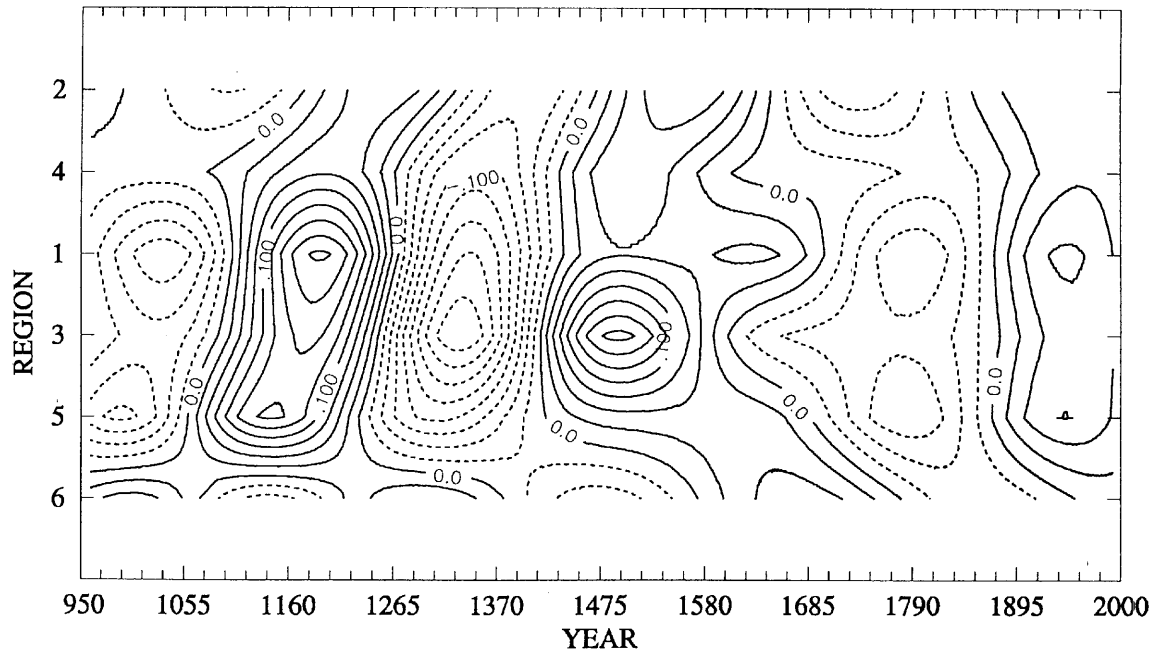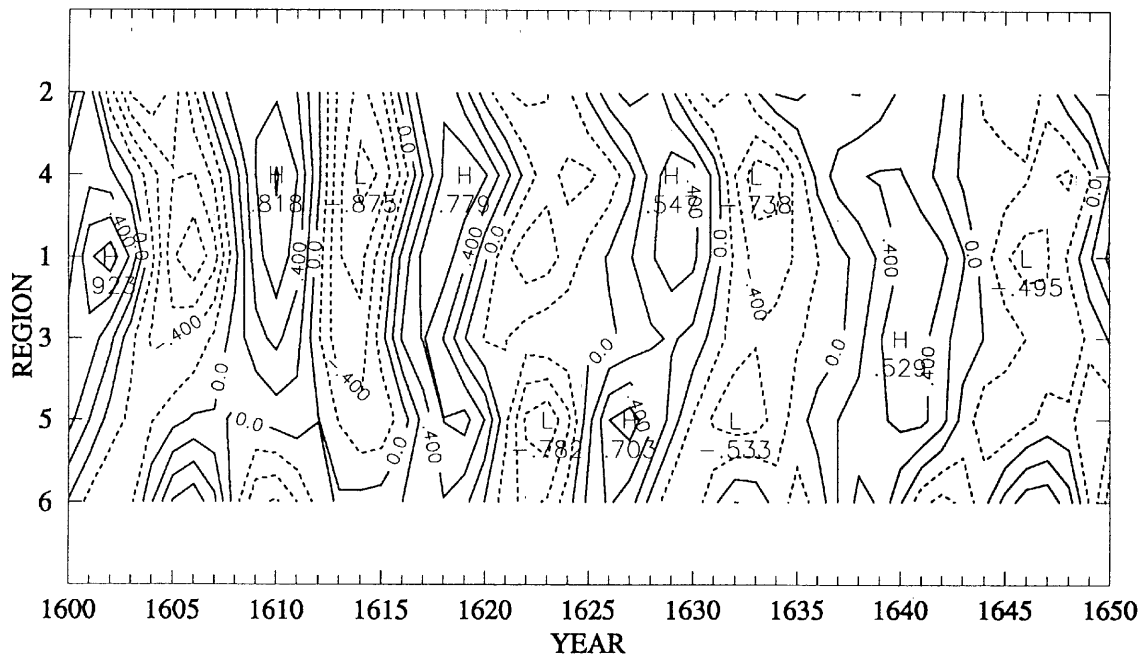
WAVELET EXPANSION AT a=80 FOR 6 REGIONS

Figure 5. The wavelet expansion on $a = 80$ years scale for the six regions

For the shorter time-scale $a = 10$ years (Figure 6), some synchronous variations still appear in some regions. For example, an almost synchronous change from a wet episode to a weak dry spell occurred around 983, with an abrupt change around 981 in region 3 (Zhang and Jiang, 1996). Other synchronous changes from a dry episode to a wet spell emerged around 1216, with an abrupt change in regions 6, 4 and 3; the abrupt change around 1644 (it was the end of the Min Dynasty, before which the well-known 'Chongzhen' severe drought spell occurred) in regions 1, 2, 3 and 4 detected by Zhang and Jiang (1996), are also displayed in this figure. In addition, the severe floods in the Yellow River basin (affecting regions 1, 3 and 4) during 1650–1663 are also noted. Furthermore, a weaker synchronous dry spell during 1930–1940, is followed by a wet spell in regions 1, 3, 5 and 6; an opposite variation is observed between regions 1, 4, 2 and 3 (north of the Huai River) and regions 6 and 5 (south of the Huai River) during the period 1840 to 1920. These have not been detected by the moving 't' test applied to identify abrupt climate changes.

Finally, two segments of the wavelet expansion on the $a = 2$ year time-scale are presented by 'zooming in' on the variations for the period from 1600 to 1650 and 1280 to 1330. Figure 7(a) is for 1600–1650. This period lies in the Little Ice Age and in a weaker dry stage detected by the longer time-scale variability analysis (see Figure 5). The fluctuation in region 4 coincides statistically with Fang's (1992) detailed example of the calamity records found in the eastern Henan Province. We still find some synchronous variabilities although with some differences in timing (year). The 'Chongzhen' severe drought covered the spell of 1636–1643 except for the two wet years in 1641–1642 in region 6. Other dry episodes around 1610, 1617–1619, and some wet episodes around 1603–1606, 1613–1615, 1621–1623, 1631–1633 and 1644–1647 are shorter and limited to parts of the regions. Figure 7(b) shows the variability for 1280–1330. This period lies at the end of the little climate warm epoch, also in the outstanding wet stage of longer time-scales in regions 1, 3 and 5 (see Figure 5). It displays few synchronous variations except for the years around 1287, 1312, 1316 and 1328–1329, in which wet or dry episodes occurred in most regions. Comparing Figure 7(b) and 7(a) shows some evidence that the droughts extend over larger areas than the floods. The fact that the overall numbers of positive and negative values of the wavelet expansion are more or less equal in both segments is due to the zero mean property of the wavelet function (equation (4) in the Appendix).

WAVELET EXPANSION AT a=10 FOR 6 REGIONS (a)

WAVELET EXPANSION AT a=10 FOR 6 REGIONS (b)

Figure 6.   As in Figure 5, but for the time-scale $a = 10$ years (b is continued from a)

WAVELET EXPANSION AT a=2 FOR 6 REGIONS (a)

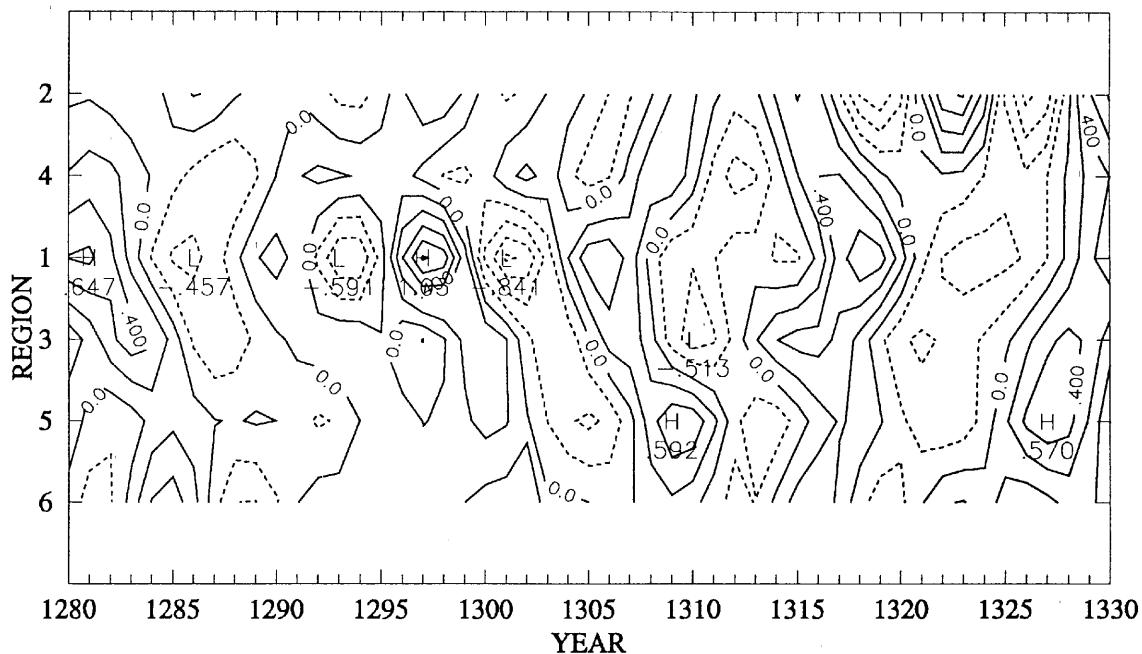## WAVELET EXPANSION AT a=2 FOR 6 REGIONS (b)

Figure 7.   As Figure 5, but for $a = 2$ year scale: (a) for the time segment 1600–1650, (b) for 1280–1330

5. SUMMARY

A data set of annual grades of wetness is analysed for six regions in East China covering the last 1033 years. Descriptive statistical analysis and application of the 'Mexican hat' wavelet transform lead to the following conclusion.

(i)   The probability distribution of occurrences of the five grades is almost normally distributed for all six regions: about 30 per cent of the probability occur on the normal grade, 23 per cent on the dry or wet grade, 12 per cent on the abnormally dry or abnormally wet grade. More droughts than floods appear in the semi-arid climate zone, whereas more floods than droughts occur in the wet climate zone.

(ii) Wavelet analysis of climatic fluctuation displays both the variations of different time-scales (or frequencies) at particular time points, and persistent anomalies. The abrupt climatic changes between the persistent anomalies also can be displayed by pairs of significant centres of the wavelet transform or expansion closing to each other with a large gradient in the symmetric wavelet transform, but statistical significance tests are required.

(iii) The climatic variations occurring on longer time-scales may cover a larger area, such as around 1110–1240 and 1270–1400 in regions 1, 3 and 5. These are the outstanding persistent dry and wet stages during the last 1033 years. An almost synchronous change since the seventeenth century occurs from a weaker wet phase to a weaker dry stage around 1890. The variation features in the former 960–1469 differ from those in the latter 1470–1992 years. On shorter time-scales, some synchronous fluctuations are also observed but in fewer years.

(iv) The variations on longer time-scales identified in this data set coincide roughly with those identified by Gong and Hameed (1991) for the period after 1060. Differences between our and their data sets for the period 960–1060 require further analysis.

APPENDIX

The 'Mexican hat' wavelet transform and reconstruction are obtained as follows: The continuous wavelet transform coefficients $W(a,b)$ of a real square integrable signal $f(x)$ with respect to a real integrable analysing wavelet $g(x)$ are defined as in Katul *et al.* (1994) and in Gao and Li (1993):

$$W(a, b) = (C_g a)^{-1/2} \int_{-\infty}^{\infty} f(t)\, g[(t - b)/a]\, \mathrm{d}t \qquad (1)$$

where $W(a,b)$ represents the wavelet transform function, or the so-called wavelet coefficients, of the raw data function $f(t)$; a ($a > 0$) is the scale parameter. A larger a value corresponds to a longer time-scale or a lower fluctuation frequency; $C_g a$ is an energy normalization term, which keeps the energy of those scaled 'daughter wavelet' equalling the energy of the 'mother wavelet'; and b is the location parameter. The C_g is defined by

$$C_g = \int_{-\infty}^{\infty} h^2(k)\mathrm{d}k/\mid k \mid < \infty \qquad (2)$$

where k is the wavenumber and $h(k)$ is the Fourier transform of $g(x)$ given by

$$h(k) = \int_{-\infty}^{\infty} g(x)\exp(-ikx)\mathrm{d}x \qquad (3)$$

The condition in equation (2) ensures the locality of C_g in the Fourier domain. The function $g(x)$ satisfies

$$\int_{-\infty}^{\infty} g(x)\mathrm{d}xz = 0 \tag{4}$$

This condition means that the area covered by the wavelet envelope is zero, and ensures that the shape of the wavelet function is always in proportion to the parameters a and b while they vary.

The 'mexican hat' function used in this study is

$$g(x) = (1 - x^2)\exp(-x^2/2) \tag{5}$$

where $x = (t - b)/a$, and defined within $-4 \cdot 0 < x < 4 \cdot 0$. In this basic wavelet function, a responds to 1/4 cycle.

The variance of a wavelet component on the time-scale a is calculated as follows:

$$V(a) = \sum_{b=1}^{N} W^2(a, b) \tag{6}$$

The raw data function $f(t)$ can be reconstructed from the wavelet coefficients by

$$f(t) = C_g^{-1/2} \int_0^\infty \int_{-\infty}^\infty a^{-1/2} g[(t - b)/a]W(a, b)\mathrm{d}b \ \mathrm{d}a/a^2 \tag{7}$$

The wavelet expansion on the time-scale a is calculated as follows:

$$y(a, t) = C_g^{-1/2} \int_0^\infty \int_{-\infty}^\infty a^{-1/2} g[(t - b)/a]W(a, b) \ \mathrm{d}b \ \mathrm{d}a/a \tag{8}$$

REFERENCES

Brunet, Y. and Collinean, S. 1994. 'Wavelet analysis of diurnal and nocturnal turbulence above a maize crop', in Foufoula-Georgiou, E. and Kumar, P. (eds), *Wavelets in Geophysics*, Academic Press, San Diego, pp. 129–150.

Chu, K.-C. 1926. 'Climate pulsations during historic times in China'. *Geogr. Rev.*, **16**, 274–281.

Chu, K.-C. (or Zhu, K.-Z. in Chinese) 1973. 'A preliminary study on the climate fluctuations during the last 5000 years in China', *Sci. Sin. (Ser. B)*, **16**, 226–256.

Fang, J.-Q. 1992. 'Establishment of a data bank from records of climatic disasters and anomalies in ancient Chinese documents', *Int. J. Climatol.*, **12**, 499–519.

Foufoula-Georgiou, E. and Kumar, P. 1994. *Wavelets in Geophysics, Wavelet Analysis and its Applications*, Vol. 4, Academic Press, San Diego, 373 pp.

Gamage, N. and Blumen, W. 1993. 'Comparative analysis of low-level cold fronts: wavelet, Fourier, and empirical orthogonal function decompositions', *Mon. Wea. Rev.*, **121**, 2867–2878.

Gao, W. and Li, B.L. 1993. 'Wavelet analysis of coherent structure at the atmosphere–forest interface', *J. Appl. Meteorol.*, **32**, 1717–1719.

Gong, G. and Hameed, S. 1991. 'The variation of moisture conditions in China during the last 2000 years', *Int. J. Climatol.*, **11**, 271–283.

Grossman, A. and Morlet, J. 1984. 'Decomposition of Hardy functions into square integrable wavelets of constant shape', *SIAM J. Math. Anal.*, **15**, 732–736.

Hagelberg, C.R. and Gamage, N.K. 1994. 'Applications of structure preserving wavelet decompositions to intermittent turbulence: a case study', in Foufoula-Georgiou, E. and Kumar, P. (eds), *Wavelets in Geophysics*, Academic Press, San Diego, pp. 45–80.

Hassan, F.A. 1981. 'Historical Nile floods and their implication for climate change', *Science*, **212**, 1142–1144.

Katul, G. G., Albertson, J. D., Chu, C. R. and Parlange, M. B. 1994. 'Intermittency in atmospheric surface layer turbulence: The orthonomal wavelet representation', in Foufoula-Georgiou, E. and Kumar, P. (eds), *Wavelets in Geophysics*, Academic Press, San Diego, pp. 81–105.

Kumar, P. and Foufoula-Georgiou, E. 1993. 'A new look at rainfall fluctuations and scaling properties of spatial rainfall using orthogonal wavelets', *J. Appl. Meteorol.*, **32**, 209–222.

Liu, P. C. 1994. 'Wavelet spectrum analysis and ocean wind waves', in Foufoula-Georgiou, E. and Kumar, P. (eds), *Wavelets in Geophysics*, Academic Press, San Diego, pp. 151–166.

Mahrt, L. 1991. 'Eddy asymmetry in the sheared heated boundary layer', *J. Atmos. Sci.*, **48**, 472–492.

Meyers, S. D., Kelly, B. G. and O'Brien, J. J. 1993. 'An introduction to wavelet analysis in oceanography and meterology: with application to the dispersion of Yanai waves', *Mon. Wea. Rev.*, **121**, 2858–2866.

Morlet, G. A., Fourgeau, I. and Giard, D. 1982. 'Wave propagation and sampling theory', *Geophysics*, **47**, 203–236.

Sheng, C. 1981. 'A preliminary analysis of the historic drought/flood records during recent 500 years', *Proceedings of Conference on Climate Change in China*, Science Press, Beijing, pp. 36–45. (In Chinese).

Spedding, G. R., Browand, F. K., Huang, N. K. and Long, S. R. 1993. 'A 2-D complex wavelet analysis of an unsteady wind-generated surface wave field', *Dyn. Atmos Oceans*, **20**, 55–77.

State Meteorological Administration of China. 1981. *Yearly Charts of Drought/Floods in China for the last 500 Years (1470–1979)*, Cartography Press of China, Beijing. (In Chinese).

Wang, R., Wang, S. and Fraedrich, K. 1991. 'An approach to reconstruction of temperature on a seasonal basis using historic documents from China', *Int J. Climatol.*, **11**, 381–392.

Wang, S. and Zhao, Z. 1981. 'Reconstruction of the summer rainfall regime for the last 500 years in China', *Geojournal*, **5**, 117–122.

Weng, H. and Lau, K. M. 1994. 'Wavelet, period doubling, and time-frequency localization with application to organization of convection over the tropical western Pacific', *J. Atmos. Sci.*, **51**, 2523–2541.

Zhang, D. 1983. 'The method and its reliability of reconstruction of the climatological series for the last 500 years', in Academy of Meteorology of the State Meteorological Administration of China (eds), *Reports of Meteorological Science and Technology (4)*, Meteorological Press, Beijing, pp. 17–26 (In Chinese).

Zhang, D. 1991. 'The relationship between the Little Ice Age climate in China and the global change', *Quatern. Res.*, **2**, 104–111 (in Chinese); or, 1994, 'The Little Ice Age climate in China', in Glaeser, P.S. and Milward, M.T.L. (eds), *New Data Challenges in our Information Age*, CODATA, Paris, pp. B67–76.

Zhang, D. and Jiang, J. 1996. 'A study of abrupt dry–wet climatic change during the last 1000 years for six regions in China', in Fu Congbin and Yan Zhongwei (eds), *The Global Change and Ecological Environment for the Future in China*, Meteorological Press, Beijing, pp. 37–44.

Zhang, D., Liu, C. and Gu, X. 1995. 'A research of reconstruction of 6 regional dry/wet grades series in the east China for the last 1000 years', *in Collections of Research Papers on Climate Change and its Numerical Simulation (1)*, Meteorological Press, Beijing, in press (in Chinese).

Zhang, J., Zhang, X. and Xu, X. 1983. 'The drought and flood in China for recent 500 years', in Academy of Meteorology of the State Meteorological Administration of China (eds), *Reports of Meteorological Science and Technology (4)*, Meteorological Press, Beijing, pp. 1–16. (In Chinese).